Received: 10 May 2019 | Revised: 1 August 2019 | Accepted: 11 August 2019

DOI: 10.1002/bit.27146

BIOTECHNOLOGY BIOENGINEERING WILEY

ARTICLE

Cell free biosynthesis of isoprenoids from isopentenol

Valerie C.A. Ward[1,2] | Alkiviadis Orfefs Chatzivasileiou[1] | Gregory Stephanopoulos[1]

[1]Department of Chemical Engineering, Massachusetts Institute of Technology, Cambridge, Massachusetts

[2]Department of Chemical Engineering, University of Waterloo, Waterloo, Ontario, Canada

Correspondence
Gregory Stephanopoulos, Massachusetts Institute of Technology, 77 Massachusetts Ave. Cambridge, MA, 02139, USA.
Email: gregstep@mit.edu

Funding information
U.S. Department of Energy, Grant/Award Numbers: DE-EE 000 7531, DE-SC 000 8744; Natural Sciences and Engineering Research Council of Canada

Abstract

Cell-free systems are growing in importance for the biosynthesis of complex molecules. These systems combine the precision of traditional chemistry with the versatility of biology in creating superior overall processes. Recently, a new synthetic pathway for the biosynthesis of isoprenoids using the substrate isopentenol, dubbed the isopentenol utilization pathway (IUP), was demonstrated to be a promising alternative to the native 2C-methyl-D-erythritol-4-phosphate (MEP) and mevalonate (MVA) pathways. This simplified pathway, which contains a minimum of four enzymes to produce basic monoterpenes and only depends on ATP and isopentenol as substrates, allows for a highly flexible approach to the commercial synthesis of isoprenoid products. In this work, we use metabolic reconstitution to characterize this new pathway in vitro and demonstrate its use for the cell-free synthesis of mono-, sesquit-, and diterpenoids. Kinetic modeling and sensitivity analysis were also used to identify the most significant parameters for taxadiene productivity, and metabolic control analysis was employed to elucidate protein-level interactions within this pathway, which demonstrated that the IUP enzymatic system is primarily controlled by the concentration and kinetics of choline kinase (CK) and not regulated by any pathway intermediates. This is a significant advantage over the natural MEP or MVA pathways as it greatly simplifies future metabolic engineering efforts, both in vitro and in vivo, aiming at improving the kinetics of CK. Finally, we used the insights gathered to demonstrate an in vitro IUP system that can produce 220 mg/L of the diterpene taxadiene, in 9 hr, almost 3-fold faster than any system reported thus far.

KEYWORDS
biocatalysis, enzyme kinetics, isoprenoids, metabolic control analysis, taxadiene

1 | INTRODUCTION

Isoprenoids are a large class of diverse molecules which encompasses high-value pharmaceuticals such as paclitaxel and low-value bulk chemicals like isoprene (Vickers, Bongers, Liu, Delatte, & Bouwmeester, 2014). While isoprenoids are produced in all organisms, many of the compounds of greatest interest are made in small quantities in plants (Vickers et al., 2014). Due to the high cost of plant procurement and recovery from plants, high-level production of isoprenoids through microbial metabolic engineering is highly desirable and significant progress has been made toward this goal with several challenges remaining, such as strict regulation (Y. Chen, Zhou, Siewers, & Nielsen, 2015; Ward, Chatzivasileiou, & Stephanopoulos, 2018) toxicity caused by over-accumulation of pathway intermediates (George et al., 2018) and low productivities.

These challenges can be addressed by using cell-free biocatalysis. Cell-free biosynthesis greatly simplifies the process by, (a) eliminating the need for extensive strain engineering, (b) removing competing metabolic pathways, such as those needed to support cell growth and viability, which erodes the maximum achievable yields, (c) alleviating transcriptional and translational regulation present in vivo, and (d) avoiding the effects of host toxicity caused by accumulation of pathway intermediates. In vitro biosynthesis of isoprenoids becomes particularly attractive when one contemplates numerous attempts

over the past years to engineer these pathways which have demonstrated that extensive engineering of central carbon metabolism is also required to achieve even moderate gains in isoprenoid titers (Meadows et al., 2016).

Yet, examples of cell-free systems used at scale are limited. This is primarily due to the high cost of enzyme production and purification, but also to the use of expensive labile cofactors which are required by many pathways. The latter is normally regenerated by complex metabolic systems in vivo which are no longer present in vitro and add significantly to the cost of cell-free biosynthesis (Dudley, Karim, & Jewett, 2015). While cofactor regeneration systems have been demonstrated for adenine triphosphate (ATP) using the low-cost substrate polyphosphate (Andexer & Richter, 2015; Mordhorst, Siegrist, Müller, Richter, & Andexer, 2017; Schwander, Schada von Borzyskowski, Burgener, Cortina, & Erb, 2016), the use of nicotinamide adenine dinucleotide (NADH) and nicotinamide adenine dinucleotide phosphate (NADPH) in cell-free systems remains a significant challenge (Dudley et al., 2015; Zhang, 2011), and these regeneration systems can lead to over-accumulation of byproducts which may limit the productivity of the system during batch operations. True cofactor recycling systems are far more complex, involving many more enzymes, however, prevent the accumulation of inhibitory byproducts (Guterl et al., 2012; Y. Wang & Zhang, 2009). The native mevalonate (MVA) and 2C-methyl-D-erythritol-4-phosphate pathways both have multiple cofactor requirements including NAD(P)H and ATP/cytosine triphosphate (CTP). Furthermore, the direct precursors to these pathways, acetyl-CoA, pyruvate, and glyceraldehyde-3-phosphate are not bulk chemicals making them unsuitable for cell-free synthesis on their own (Boronat & Rodríguex-Concepción, 2015). To use a low-cost feedstock like glucose, glycolysis enzymes must also be included along with terpene pathway enzymes to precisely balance cofactor generation and utilization steps. This was demonstrated for the production of monoterpenes, which required 27 enzymes to sustainably synthesize monoterpenes from glucose (Korman, Opgenorth, & Bowie, 2017). While they were able to achieve high titers (>11 g/L over 7 days) of pinene, sabinene, and limonene, and mitigate the toxicity effects which limit monoterpene production in vivo, the high cost for the production, purification, and maintenance of so many enzymes would be prohibitive at scale.

Recently a new synthetic pathway for the production of isoprenoids was reported, the isopentenol utilization pathway (IUP; Chatzivasileiou et al., 2019), elements of which had also been investigated in previous works (Lange & Croteau, 1999; Wang et al., 2018). This pathway converts the substrates prenol or isoprenol to isoprenyl pyrophosphate (IPP) and dimethylallyl pyrophosphate (DMAPP), respectively, through two phosphorylation reactions catalyzed by the enzymes choline kinase (CK; Chatzivasileiou, Ward, Edgar, & Stephanopoulos, 2019) and isopentenyl phosphate kinase (IPK; Lange & Croteau, 1999; Figure 1). This pathway was characterized in vivo and achieved high flux with very little optimization. Using the IUP for cell-free monoterpene biosynthesis would dramatically shorten the pathway to only four enzymes (CK, IPK, farnesyl diphosphate synthase [IspA], and a monoterpene synthase) so that the synthesis of even complex cyclic diterpenes like taxadiene would only require five enzymes. A cell-free IUP could have significant potential for commercial production of isoprenoids, particularly for high-value compounds.

Finally, cell-free systems can also be used to study pathway kinetics and elucidate rate-limiting steps using a systematic approach to guide the optimization of metabolic pathways in vivo (Galloway, Laimins, Division, & Hutchinson, 2015; Guo, Sheng, & Feng, 2017). They can identify the most significant factors that control the overall flux of the pathway or to identify pathway regulatory mechanisms at the protein level (Guo et al., 2017; Zhu et al., 2014). The MVA pathway starting at MVA and acetyl-CoA has been well studied using this method for the production of amorphadiene (X. Chen, Zhang, Zou, Stephanopoulos, & Too, 2017) and farnesene (Zhu et al., 2014). These studies identified previously unknown regulatory interactions and rate-controlling steps which were successfully used to improve the pathway flux in vivo.

In this work, the kinetic properties of our pathway enzymes were elucidated in vitro and the cell-free synthesis of limonene, valencene, amorphadiene, and taxadiene using the IUP was demonstrated. To optimize the fraction of each enzyme required to achieve the highest pathway flux, a large perturbation study of the effect of enzyme concentration on the overall pathway flux and the concentration of metabolic intermediates was performed and analyzed. Metabolic control analysis (MCA) was employed to elucidate the sensitivity of each enzyme towards pathway metabolites and identify enzymes strongly regulated by pathway intermediates. This information was used to determine the optimal fraction of each enzyme to achieve the highest flux towards taxadiene production. The system was then further studied by constructing an ordinary differential equation (ODE) model based on previously reported kinetics of the IUP enzymes and those determined in this study. Rate laws were constructed using "convenience rate laws" (Liebermeister & Klipp, 2006) and global sensitivity analysis was used to determine the parameters (enzyme concentration, substrate affinity, and catalytic constants) with the highest impact on taxadiene production. Lastly, the effects of process parameters such as ATP and magnesium concentration on taxadiene production were investigated. Along with the possibility of using multiple substrates (prenol/isoprenol) in lieu of including the enzyme isopentenyl diphosphate isomerase (IDI) for their interconversion, the scalability of the cell-free system was studied ultimately achieving biosynthesis of taxadiene with high productivity.

2 | MATERIALS AND METHODS

2.1 | Strains and cultivation conditions

The gene for *CK* from *Saccharomyces cerevisiae* was previously codon-optimized for expression in *Escherichia coli*, 6× his-tagged and cloned under the control of the $T7_{lacUV}$ promoter in pET28a(+) for overexpression in *E. coli* BL21 (DE3; Chatzivasileiou et al., 2019).

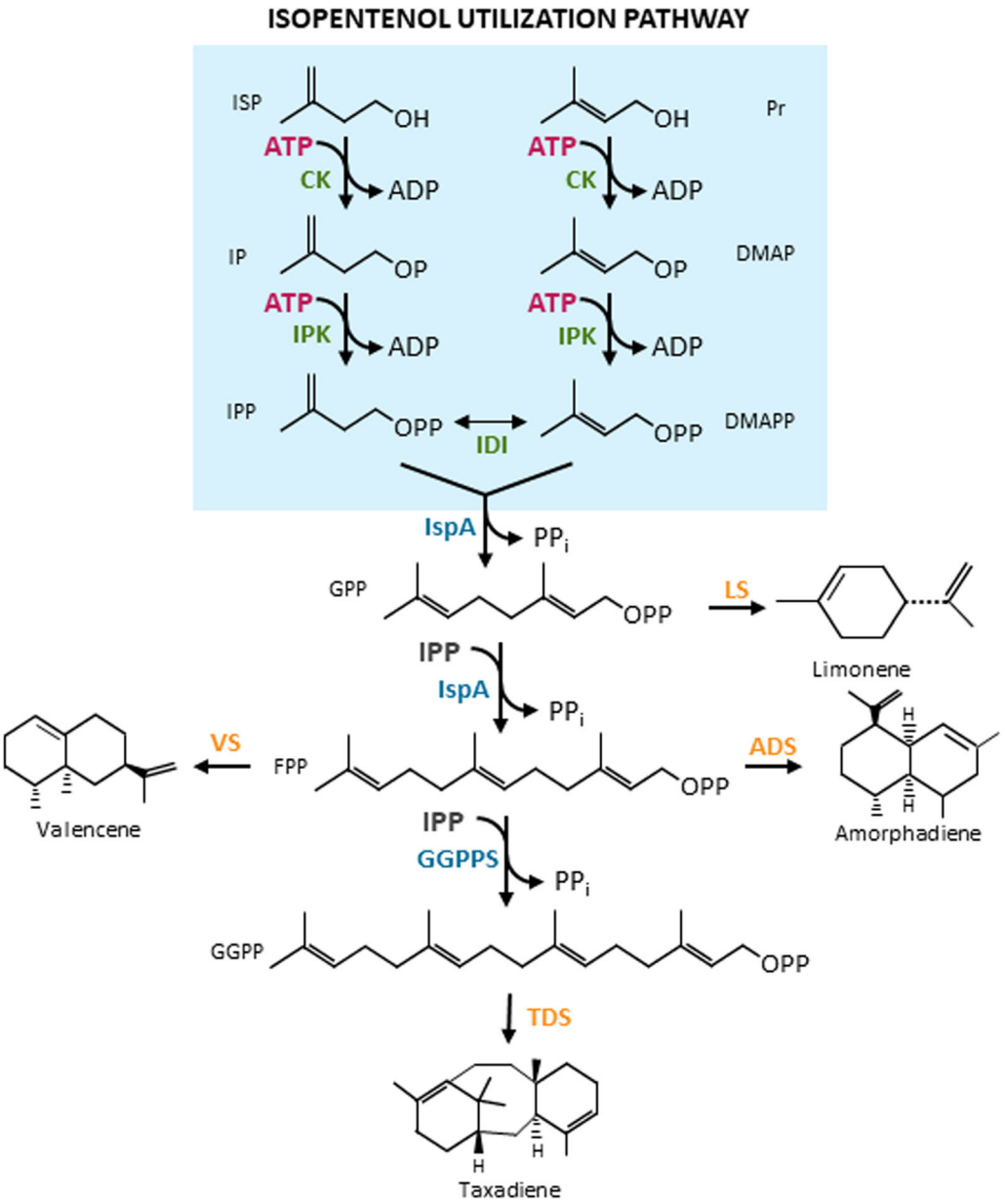

FIGURE 1 Reaction scheme for the synthesis pathway for taxadiene, valencene, amorphadiene, and limonene starting from isoprenol or prenol. The box indicates the enzymes of the IUP. Enzymes involved in the IUP include choline kinase (CK), isopentenyl phosphate kinase (IPK), and isopentenyl pyrophosphate isomerase (IDI). Enzymes from the terpenoid backbone biosynthesis pathway used in this work are shown in blue and include farnesyl pyrophosphate synthase (IspA), and geranylgeranyl pyrophosphate synthase (GGPPS). Terpene synthases used in this work are shown in orange and include limonene synthase (LS), valencene synthase (VS), amorphadiene synthase (ADS), and taxadiene synthase (TDS). Metabolites structures are shown in black and include: isoprenol (ISP), prenol (Pr), adenosine triphosphate (ATP), adenosine diphosphate (ADP), isoprenyl phosphate (IP), dimethylallyl phosphate (DMAP), isoprenyl pyrophosphate (IPP), dimethylallyl pyrophosphate (DMAPP), geranyl pyrophosphate (GPP), farnesyl pyrophosphate (FPP), and geranylgeranyl pyrophosphate (GGPP). IUP, isopentenol utilization pathway [Color figure can be viewed at wileyonlinelibrary.com]

The following genes were also cloned into pET28a(+) and his-tagged for overexpression and purification: isopentenyl kinase (*ipk*) from *Arabidopsis thaliana*, isopentenyl pyrophosphate isomerase (*idi*) from *E. coli*, farnesyl pyrophosphate synthase (*ispA*) from *E. coli*, geranylgeranyl pyrophosphate synthase (*ggpps*) from *Taxus canadensis* (Ajikumar et al., 2010), a truncated taxadiene synthase (*tds*) from *Taxus brevifolia* (Ajikumar et al., 2010), a codon-optimized amorphadiene synthase (*ads*) from *Artemisia annua* (Martin, Pitera, Withers, Newman, & Keasling, 2003), a valencene synthase (*vs*) from *Callitropsis nootkatensis* (Yang, Sau, Lai, Cichon, & Li, 2015), and a limonene synthase (*ls*) from *Mentha spicata* (Alonso-Gutierrez et al., 2013). All plasmids were constructed using a standard workflow for Gibson assembly described in our previous work (Chatzivasileiou et al., 2019). Detailed information on plasmids and primers is given in the Supporting Information data (Table S1–2). Plasmids were constructed by amplifying the pET28a vector backbone and

amplifying each enzyme sequence. Gibson assembly was used to assemble the vector backbone and each gene to create nine separate plasmids encoding one enzyme each under the control of a $T7_{lacUV}$ promoter followed by a 6× His-tag and the T7 terminator region. Plasmids were confirmed by sequencing then were transformed by heat-shock into BL21 (DE3) according to manufacturer's recommendation (New England Biolabs, [NEB]) and plated on kanamycin plates (50 μg/L) overnight at 37°C. The list of plasmids used in this study is reported in Table S1 and primer sequences used are listed in Table S2.

2.2 | Cultivation, protein expression, and quantification

A single colony from each strain containing one plasmid for the expression of a single enzyme was inoculated into 5 ml of sterile luria broth (LB) media (BD Sciences) with kanamycin and grown overnight at 37°C. One milliliter was then inoculated into a 1 L flask containing 200 ml of sterile super optimal broth (SOB) media (AMRESCO, Inc.) with kanamycin. The culture was grown at 30°C until an optical density of 0.4–0.6 (λ = 600 nm). At this point, protein production was induced by the addition of isopropyl-β-D-thiogalactoside (IPTG) for a final concentration of 0.1 mM and continued at 30°C for 3 hr. Cells were harvested by centrifugation at 3750 rpm in an Allegra X-12R centrifuge (Beckman Coulter). The supernatant was removed and the cell pellets were frozen at −20°C until purification. Proteins were visualized by sodium dodecyl sulfate-polyacrylamide gel electrophoresis performed according to the manufacturer's guidelines (Bio-Rad). Gradient (4–20%) gels were purchased from Bio-Rad, as were the kaleidoscopes prestained protein ladder, Laemelli 4× sample buffer, Tris-glycine-SDS buffer, and mini-protean electrophoresis chambers. Gels were stained using Instant-Blue (Expedeon). Protein concentrations were very roughly estimated from the gel using ImageJ (NIH) to determine an appropriate amount of resin for purification.

2.3 | Protein purification

All purification steps were performed in a single day on ice and in a cold room when possible. Cell pellets were thawed and resuspended in 30 ml of NPI-10 buffer (50 mM NaH_2PO_4, 300 mM NaCl, 10 mM imidazole, pH 8.0) and supplemented with 0.5 mM phenylmethylsulfonyl fluoride (PMSF) immediately before cell lysis. Cells were lysed by passaging 2–3 times through an EmulsiFlex-C5 high-pressure homogenizer (Avestin). Lysates were then centrifuged at 4°C for 15 min to remove cellular debris. The clarified lysate was loaded onto a Ni-NTA resin (Gold Bio, capacity 50 mg/mL) which was housed in a gravity column (Thermo Fisher Scientific) and was preequilibrated with 10 column volumes (CV) of NPI-10 buffer. The column was then washed with 10 CV of NPI-20 buffer (20 mM imidazole). The enzyme was then eluted from the column by three CV using NPI-250 buffer (250 mM imidazole). Enzymes were exchanged into 50 mM Tris-Hydrochloric acid (HCl) pH 7.5 using 10 kDa Microseps (Millipore) by centrifugation and repeated buffer exchanges until the imidazole was calculated to be under 1 mM. Buffer exchange of IDI was performed by using a 10 kDa Float-a-lyzer device (Spectrum Labs) for dialysis as the solution would not exchange through the Microsep. In this case, the IDI solution was added to the Float-a-lyzer and the solution was topped up to 10 ml using 50 mM Tris (pH 7.5). The device was placed fully submerged in a beaker of 50 mM Tris (pH 7.5) and the buffer was completely changed at 2, 6, and 16 hr. Dialysis was allowed to proceed for 24 hr. Enzyme concentration was determined using a bicinchoninic acid assay kit from Pierce using bovine serum albumin as a standard (BSA). Proteins were then diluted in Tris buffer if necessary and aliquoted into microtubes which were flash-frozen in liquid nitrogen and stored at −80°C until use.

2.4 | Individual enzyme assays

To estimate the best ratio of pathway enzymes, each enzyme's activity was individually measured using a kinetic assay to determine the Michaelis–Menten constant and the specific velocity/catalytic constant (K_{cat}) of each enzyme. The kinetics for CK toward isoprenol and prenol were previously determined (Chatzivasileiou et al., 2019). The kinetics for IPK were determined by ATP consumption using a pyruvate kinase (PK) lactate dehydrogenase (LDH) coupled assay. The following components were added into a single solution then distributed into a 96 well microplate for continuous monitoring at 340 nm: 10 mM ATP, 10 mM $MgCl_2$, 50 mM ammonium bicarbonate pH 7.4, 10 mM phosphoenolpyruvate (pH 7.4), 0.6 mM NADH, and 1U of PK, and 1.4U LDH (PK-LDH solution from Sigma-Aldrich), IPK (10 μg/ml). NADH was made fresh each time and the appropriate concentration was determined by constructing a standard curve using a SpectraMax M3 plate reader and selecting the highest value in the linear range. This curve was also used to determine the adsorption coefficient of NADH for calculation of the reaction rate. The reactions were monitored before the addition of the substrate to determine if any nonspecific rate of ATP hydrolysis was present, however, there was no nonspecific ATP hydrolysis found for purified enzymes. Pyruvate and ADP (Sigma-Aldrich) were used to determine the appropriate amount of PK-LDH solution (Sigma-Aldrich) and to confirm the assay was working appropriately. No substrate/enzyme only and no enzyme/substrate only controls were also included but no activity was detected. The substrates (IP or DMAP) were diluted in a 2 log standard curve which were then added to the microplate using a multichannel pipette and NADH oxidation to NAD+ was monitored at 340 nm. Assays were done in triplicate. The rate of IPP or DMAPP formation was equivalent to the negative rate of ATP consumption. The activity of geranylgeranyl pyrophosphate synthase (GGPPS) was determined by the conversion of IPP and farnesyl pyrophosphate (FPP) to GFPP by monitoring pyrophosphate (PPi) formation using the EnzChek pyrophosphate assay kit (Invitrogen). The activity of taxadiene synthase (TDS) was also monitored using the PPi assay but only used GGPP as the substrate. The assays were performed as described for IPK using the same controls as above: TDS was added to 50 mM Tris-HCl pH 7.5, with 10 mM $MgCl_2$, 20 mM 2-amino-6-mercapto-7-pethylpurine (MESG), purine

nucleoside phosphatase, and 0.03 U of inorganic pyrophosphatase (IPPase). The substrates for GGPPS, IPP, and FPP, were each diluted in a microplate so that all combinations of each level were assayed in triplicate. The substrates were added to the appropriate well and the reaction was monitored for the fluorescence of MESG-phosphate. A standard curve was constructed using sodium pyrophosphate provided in the kit and was used to calculate the rate for each reaction. The rate of IDI was not determined as the isomerization of IPP to/from DMAPP cannot be measured using a kinetic assay and was not found to be a necessary component of the enzyme system. IspA kinetics were estimated from the literature (Ku, Jeong, Mijts, Schmidt-Dannert, & Dordick, 2005; Weaver et al., 2015).

2.5 | Multienzyme reactions in solution

The multienzyme system reactions were carried out in 50 mM ammonium bicarbonate (pH 7.4) with 10 mM $MgCl_2$, 2 mM $MnCl_2$, 0.05% (w/v) Tween 20, 10 mM ATP, and 5 mM isoprenol at 30°C unless otherwise stated. The solution in glass GC vials (Agilent) was overlaid with 1/10 volume of dodecane to entrap the volatile isoprenoids. The enzyme concentrations and raw data obtained in the large perturbation experiment are reported in Table S3. An initial estimated optimal concentration of each enzyme was calculated by balancing the rates (based on their k_{cat}) which were determined by individual enzyme assays. The final optimized enzyme concentrations were determined to be 25 μg/ml CK, 15 μg/ml IPK, 25.4 μg/ml IDI, 37.15 μg/ml IspA, 8.15 μg/ml GGPPS, and 25 μg/ml for TDS.

Time profiles were constructed by dividing up three separately prepared reaction master mixes into 100 μl aliquots in a deep-well microplate after the addition of ATP to start the reaction. The reactions were stopped at different times by the addition of 1 ml of −20°C acetonitrile which was then transferred into a microtube and centrifuged at 16,000*g* for 10 min to remove the precipitated enzymes. The supernatant was dried using a Reacti-Therm III with filtered air in glass test tubes. The dried precipitate was resuspended in 100 μl of liquid chromatography mass spectrometry (LC-MS)/MS mobile phases as described below. The samples were vortexed and then centrifuged at 16,000*g* a second time. Samples were analyzed using LC-MS/MS and/or GC-MS.

2.6 | Metabolite quantification using LC-MS/MS

Liquid chromatography was performed using an Agilent 1100 Series high performance liquid chromatography (HPLC) (Agilent Technologies) and the MS/MS was conducted using an API 4000 triple quadrupole mass spectrometer (SCIEX) with ESI running in negative MRM mode as previously described (Chatzivasileiou et al., 2019). The LC-MS/MS was equipped with an Xbridge C18 column (150 mm, 3.5 μm, 2.1 mm) from Waters and was operated using a mobile phase (A) of 0.1% v/v TBA, 0.12% v/v acetic acid, and titrated with ~0.5% v/v 5 N NH_4OH until a pH of 8.5 was reached. The elutant, acetonitrile (B) was introduced using the following gradient: 0–5 min 0% B, 5–20 min 0–65% B, 20–25 min 65% B, 25–30 min 100% B, 30–35 min 100% B, 35–36 min 100–0% B, 0% B until 45 min. Standard curves were generated for a mixture of IP, DMAPP, GPP, FPP, and GGPP diluted in mobile phase A. Standards were purchased from Sigma-Aldrich and/or Cayman Chemicals, except IP which was synthesized as previously described (Chatzivasileiou et al., 2019). The isomers IP and DMAP were determined together as total IP/DMAP as these isomers could not be resolved using this method. This also applied to the isomers IPP/DMAPP which eluted together and are indistinguishable by mass. Metabolite specific ionization and fragmentation voltages determined from a 1 μM standard solution of each metabolite was obtained using the Analyst software (v 1.6) and monitored during chromatography. Peaks were integrated using the Analyst software.

2.7 | Quantification of volatile isoprenoids

Taxadiene, valencene, amorphadiene, and limonene were quantified by diluting the dodecane overlays into an appropriate range depending on analyte concentration with ethyl acetate containing 90 mg/L caryophyllene as an internal standard as previously described (Chatzivasileiou et al., 2019). The samples were separated using an HP-5 MS UI capillary column (30 m, 250 μm, 0.25 μm; Agilent Technologies) using a 7890B Series GC and a 5977B MS. Chromatography was performed under the following conditions: 1 μl splitless injection, inlet temperature 280°C, constant inlet pressure 115.8 kPa, valve temperature 300°C, and MS transfer line 300°C. An oven program of 100°C, hold 1 min, 15°C/min until 200°C, hold 2 min, 30°C/min until 250°C, hold 1 min, and 30°C/min until 290°C, hold 2 min was used for determination of taxadiene, valencene, and amorphadiene. Limonene was separated using an oven program of 80°C, hold 3 min, 10°C/min until 140°C, hold 2 min, 45°C/min until 290°C, hold 1 min. The MS was operated at an ion source temperature of 280°C, and a quadrupole temperature of 180°C. Ions were scanned between a mass of 40–400 at 1.562 u/s. Taxadiene was quantified using a standard curve based on the m/z 122 ion which has the greatest abundance in unlabeled taxadiene. The remaining compounds were estimated by normalizing their area to that of the internal standard. The taxadiene standard was purified as previously described (Chatzivasileiou et al., 2019).

2.8 | Modeling and statistical analysis

Multiple linear regression of the small perturbation study was performed in Design Expert (Stat Ease) using main effects and intercept model where the dependent variable was GGPP flux and the independent variables were the enzyme concentrations (CK, IPK, IDI, IspA, GGPPS; Figure 2a). The enzyme concentrations were then optimized numerically to maximize GGPP flux.

Elasticities were calculated using the data obtained in the large perturbation study available in Table S3. Elasticities were calculated using the framework based on lin-log enzyme kinetics developed by Wu, Wang, Winden, Gulik, and Heijnen (2004):

(a)

	Enzyme Concentrations (μg/mL)				
Level	**CK**	**IPK**	**IDI**	**IspA**	**GGPPS**
Low	25	0.61	25	25	0.33
Medium	125	3.03	125	125	1.64
High	625	15.2	625	625	8.18

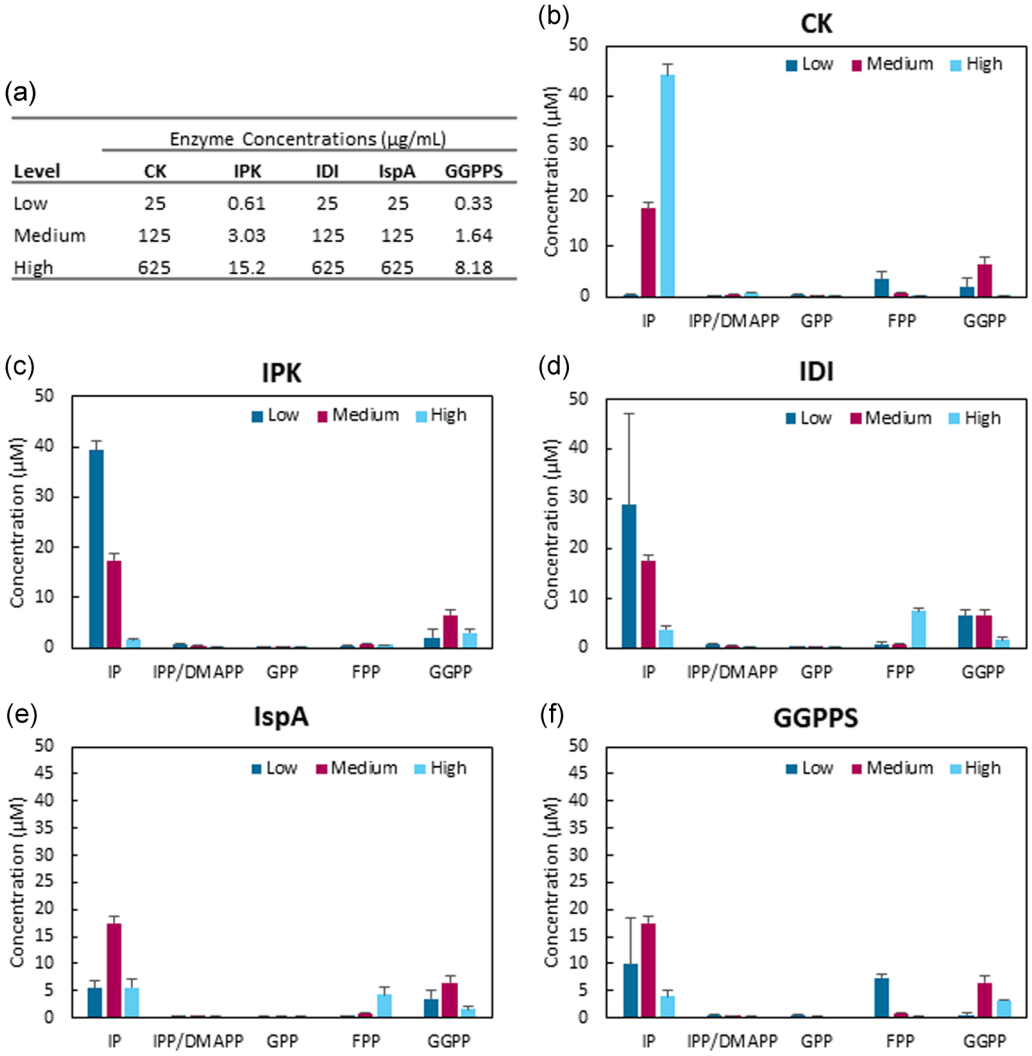

FIGURE 2 Monothetic modulation of each enzyme concentration for CK, IPK, IDI, IspA, and GGPPS. Each enzyme was modulated separately to high, low, and medium levels while all other enzymes were kept at the midpoint. Assays were conducted at 30°C, at pH 7.4 for 24 hr with 10 mM ATP and 5 mM isoprenol. All experiments were performed in triplicate (error bars 1σ). CK, choline kinase; GGPPS, geranylgeranyl pyrophosphate synthase; IPK, isopentenyl phosphate kinase [Color figure can be viewed at wileyonlinelibrary.com]

$$\frac{\mathbf{v}}{\mathbf{J^0}} = \left[\frac{\mathbf{e}}{\mathbf{e^0}}\right] \bullet \left(\mathbf{i} + \mathbf{E^{x0}} \bullet \ln\left(\frac{\mathbf{x}}{\mathbf{x^0}}\right)\right),$$

where i represents the unit vector, v represents the relative flux compared with the reference state flux J^0, E^{xO} represents the elasticity matrix for the metabolic intermediate concentrations (x^0) in relation to the enzyme concentration compared with the reference state as designed by e/e^0 and the relative intermediate metabolic concentrations compared with the reference state (x/x^0). The reference state was cycled through all 25 possible combinations used and 25 sets of elasticities were generated using the maximum connectivity assumption. The adjusted coefficient of determination (R^2) was used to determine the best reference state.

Simulation and analysis were performed in Matlab using Simulink. K_m and k_{cat} values were determined using in vitro enzyme assays described above were possible, or were determined using literature obtained through the BRENDA database, see Table 1. A full description of the model construction and mathematical representation of all rate laws are provided in the Supporting Information materials. Time course analysis using the starting conditions reported for the optimized enzyme system (10 mM ATP, 5 mM isoprenol, and 0 mM for all other species), and the enzyme concentrations (mM) used in the optimized system at 10-fold increased concentration (CK 1.88E-03, IPK 4.20E-03, IDI 1.04E-02, IspA 5.78E-03, GGPPS 1.27E-03, TDS 2.72E-03). A time course of 9 hr was used for the simulation time and nonlinear regression was used to fit the seven k_{cat} constants by minimizing the difference between the experimental time course data reported for the scalability study (Figure 6) and the simulated results. For the sensitivity analysis, a Monte Carlo simulation ($n = 500$) was used to generate taxadiene concentrations at 2 hr using a global parameter scan of all variables in the ranges reported in Table S4. The results were analyzed using multiple linear regression with stepwise elimination for variables $p > .001$.

TABLE 1 Kinetic parameters determined for the enzymes encompassing the IUP, terpenoid backbone synthesis pathway, and taxadiene synthase

Enzyme	Origin	Substrate(s)	k_{cat} (s^{-1})	K_m (μM)	Reference
Choline kinase (CK)	*Saccharomyces cerevisiae*	ISP + ATP	8.2E-03	ISP, 4,538	Chatzivasileiou et al. (2019)
		Pr + ATP	6.3E-04	Pr, 1,114	
		ATP	–	ATP, 140	Brostrom and Browning (1973)
Isopentenyl pyrophosphate kinase (IPK)	*Arabidopsis thaliana*	IP + ATP	0.013	IP, 21.7	This study
		DMAP + ATP	0.015	DMAP, 35.5	
		ATP	–	43.5	This study
Isopentenyl delta isomerase (IDI)	*Escherichia coli*	IPP/DMAPP	0.33	IPP, 9.5 DMAPP, 14.3	Hahn, Hurlburt, and Poulter (1999))
Farnesyl pyrophosphate synthase (IspA)	*E. coil*	IPP + DMAPP	0.21	DMAPP, 1.3 IPP, 29.3	Ku et al. (2005); Weaver et al. (2015)
		IPP + GPP	0.47	GPP, 10.3 IPP, 5.5	
Geranylgeranyl pyrophosphate synthase (GGPPS)	*Tsuga canadensis*	IPP + FPP	0.015	IPP, 13.5 FPP <1	This study
		IPP + FPP	3.3	FPP, 26 IPP, 39	Burke and Croteau (2002)
		3 IPP + DMAPP	1	DMAPP, 127 IPP, 88	
		2 IPP + GPP	2.1	IPP, 122 GPP, 7.7	
Taxadiene synthase (TDS)	*Taxus brevolia*	GGPP	6.4E-03	43.0	This study

Abbreviations: DMAPP, dimethylallyl pyrophosphate; FPP, farnesyl pyrophosphate; GPP, geranyl pyrophosphate; IPP, isoprenyl pyrophosphate; ISP, isoprenol; IUP, isopentenol utilization pathway; Pr, prenol.

3 | RESULTS AND DISCUSSION

3.1 | Individual enzyme kinetics

To guide the rational design of the in vitro enzyme system and aid in the construction of the kinetic model of the IUP, we first sought to determine the Michaelis–Menten kinetics for each enzyme (Table 1). As previously reported (Chatzivasileiou et al., 2019), CK shows a distinct preference for isoprenol as a substrate rather than prenol with three times greater specificity constant (k_{cat}/K_m) for isoprenol versus prenol. What is most notable is the need to have very high substrate concentrations to achieve high conversion rates (K_M = 4.5 mM) which is of a different magnitude to the other enzymes used in this study. This is likely due to the fact that isoprenol is not the natural substrate for CK, as this enzyme has an approximately 150-fold higher turnover towards choline (k_{cat} = 2.55 per subunit; Kim, Voelker, & Carman, 1997). The Michaelis–Menten parameters for IPK were estimated for IP, DMAP, and ATP as substrates (Figure S1). IPK exhibited only marginally greater affinity for IP than DMAP. GGPPS exhibited Michaelis–Menten-like behavior for its substrate IPP when FPP was held at 100 μM (Figure S1C), however, interestingly no substrate effect was detected for FPP concentrations in the range of 1–50 μM in the presence of 100 μM IPP. It has been reported elsewhere that the K_M for IPP and FPP, respectively, were 26 and 7 μM for GGPPS from *Taxus canadensis* (Burke & Croteau, 2002), which is similar to our results of 13.5 μM. In Burke and Croteau, it was also reported that GGPPS can use several combinations of substrates to form GGPP including DMAPP + 3 IPP, GPP + 2 IPP, and FPP + IPP. TDS was found to have the lowest k_{cat} of all of the enzymes used in this study (Figure S1D).

3.2 | Cell-free isoprenoid production using the multienzyme system

Since the substrates of the IUP, isoprenol, and prenol, are alcohols we were concerned that the reaction media may cause our enzymes to precipitate, therefore, we decided to first confirm that the cell-free enzyme system would be functional in an aqueous/isopentenol system. A preliminary experiment was conducted overnight by resuspending all enzymes (including IDI) at 50 μg/ml each, adding 10 mM ATP and 5 mM isoprenol, prenol, or both at a 3:1 molar ratio, and using different terpene synthases (and in the case of TDS, GGPPS was included). By supplying both isoprenol and prenol, we hoped to circumvent the need for a functional IDI in case this enzyme was inactive. We used a dodecane layer to accumulate and concentrate the isoprenoids, from which we quantified them using GC-MS (Figure S2A). In addition, we monitored the formation of the intermediates IP, IPP/DMAPP, GPP, FPP, and GGPP using LC-MS/MS (Figure S2B). All of the expected products were identified by their electron ionization mass spectra using purchased standards (valencene and limonene), a standard purified in-house (taxadiene), or from the literature (amorphadiene; Malhotra et al., 2016) and the MS spectra of the formed products are shown in Figure S2C–F. At the concentrations used, what we suspect was protein precipitation was

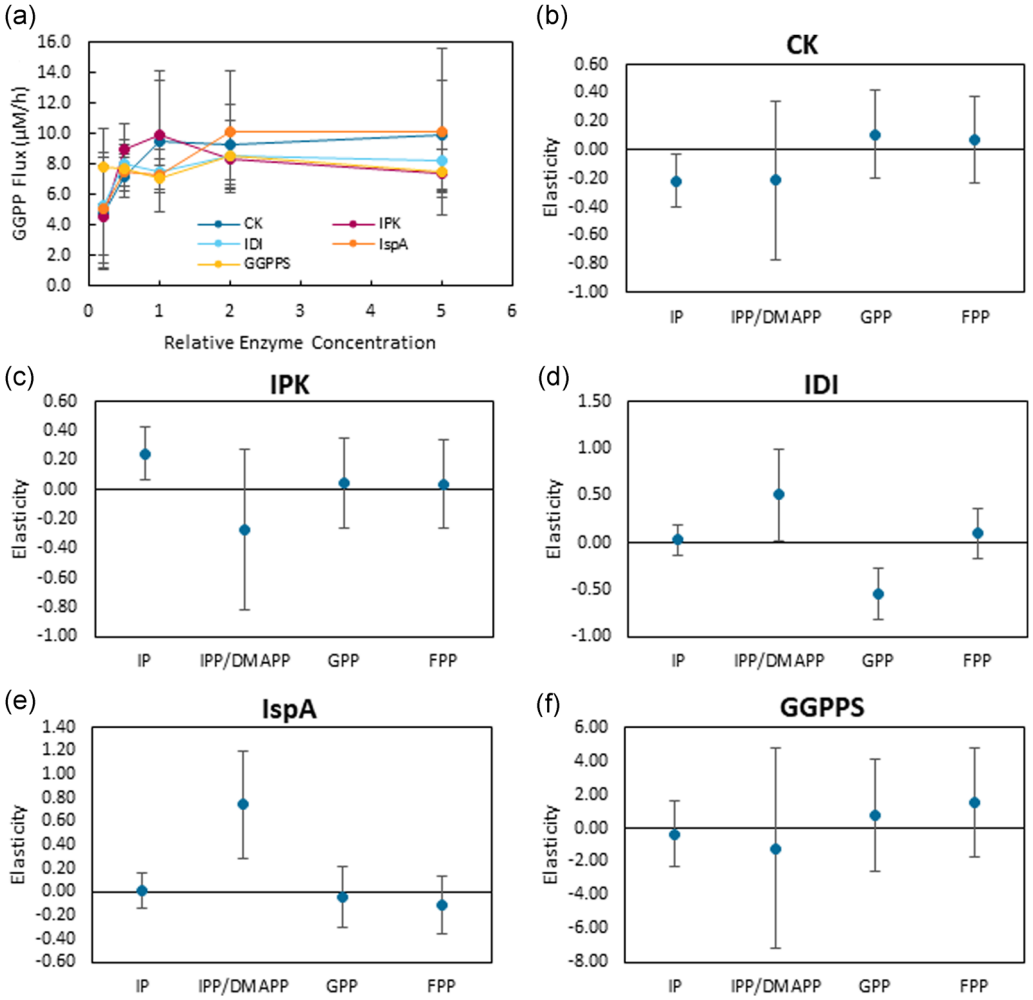

FIGURE 3 Elasticities of enzymes to pathway intermediates. (a) GGPP flux for each combination of enzyme level. Midpoint concentration of each enzyme is scaled to 1. (b–f). Elasticities calculated for the multisystem pathway using lin-log kinetics in reference to State 3 using the maximum connectivity assumption. All experiments were performed in triplicate (error bars 1σ). GGPPS, geranylgeranyl pyrophosphate synthase [Color figure can be viewed at wileyonlinelibrary.com]

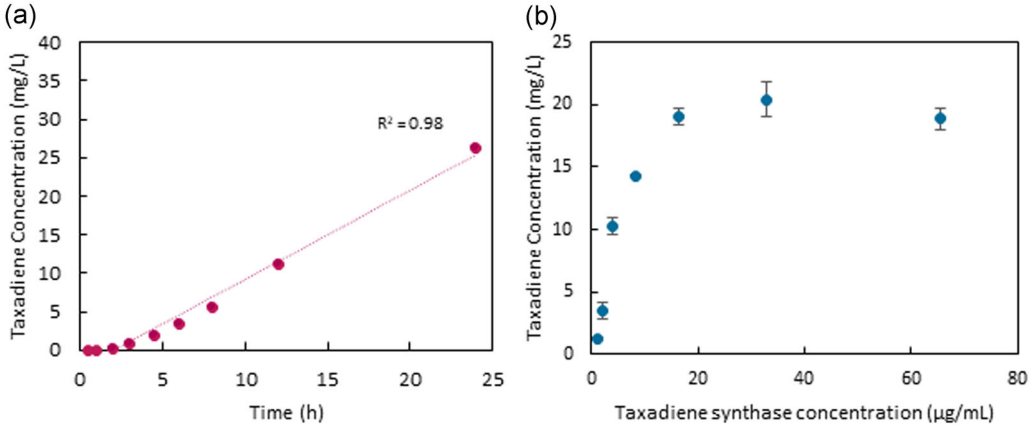

FIGURE 4 Time profile and TDS optimization for the multienzyme system. Assays were conducted at 30°C at pH 7.4. Error bars are shown for experiments performed in triplicate (1σ). (a) The linear relationship between taxadiene concentration and time. (b) Optimization of TDS concentration. All experiments were performed in triplicate (error bars 1σ). TDS, taxadiene synthase [Color figure can be viewed at wileyonlinelibrary.com]

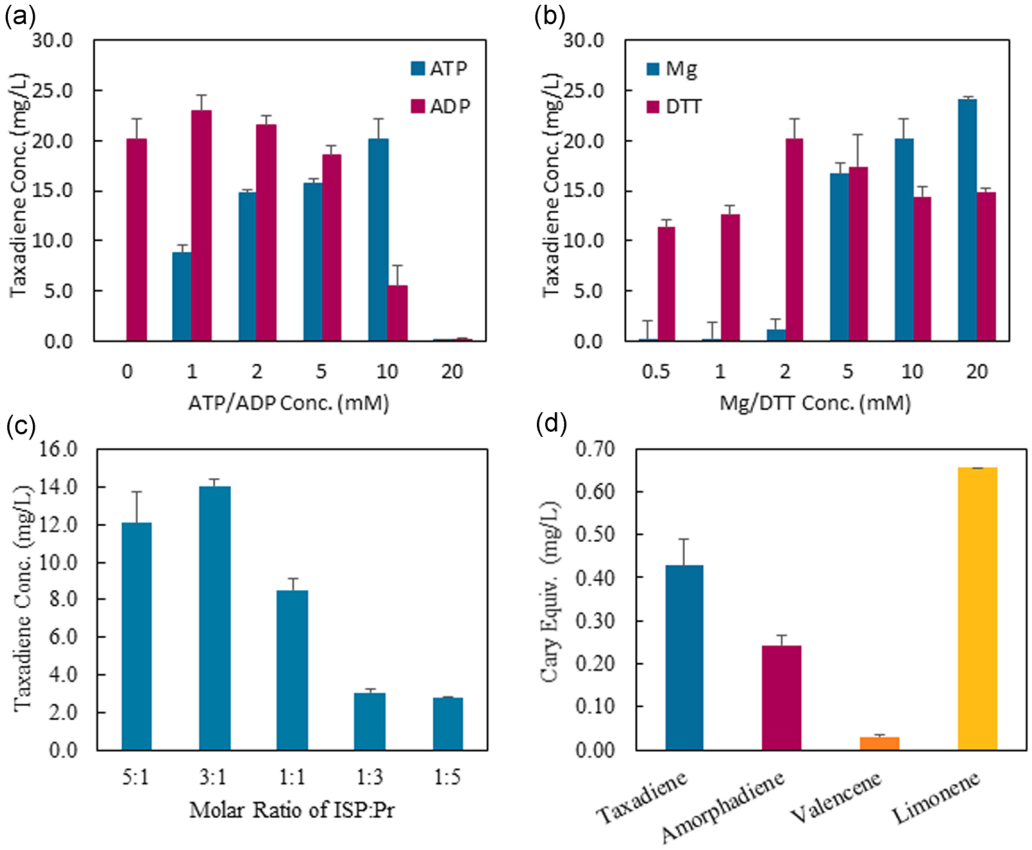

FIGURE 5 Titration of cofactors, potential inhibitors, and additives. (a) Inhibition by ATP or ADP. ATP concentration was varied from 0 to 20 mM. ADP concentration was varied from 0 to 20 mM in the presence of 10 mM ATP. (b) The dependence of the reaction on the metal ion, magnesium or on the reducing agent, DTT. (c) Varying of the isoprenol to prenol molar ratio in the multienzyme system without IDI. (d) The production of various isoprenoids using the optimized enzyme system. All experiments were performed in triplicate (error bars 1σ) [Color figure can be viewed at wileyonlinelibrary.com]

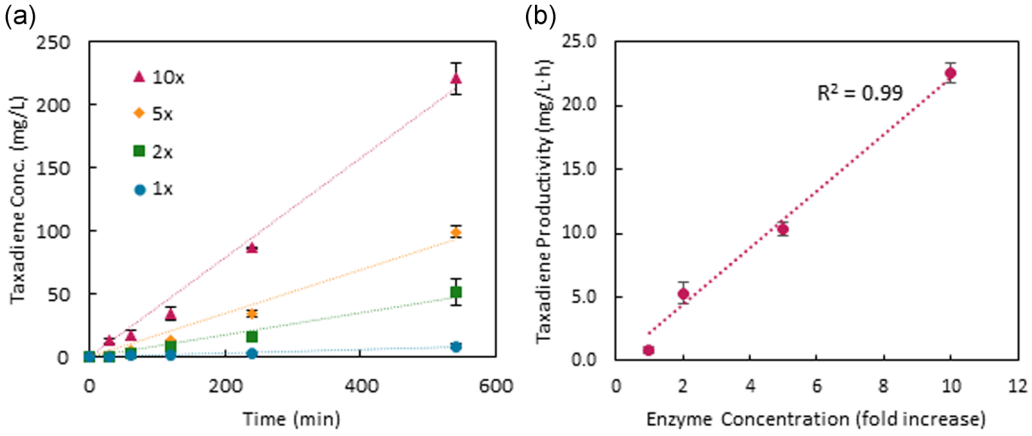

FIGURE 6 Scale-up of the optimized enzyme ratio. (a) Time profiles over 9 hr for taxadiene production. Enzymes were resuspended at either 1× (the optimized concentration), or every enzyme was resuspended at 2, 5, or 10 fold the original concentration. (b) The linear response of enzyme concentration to taxadiene flux. All experiments were performed in triplicate (error bars 1σ) [Color figure can be viewed at wileyonlinelibrary.com]

visible after 24 hr, but was prevented by the addition of 0.025% Tween 20 (w/v; data not shown) in subsequent experiments.

All the synthases used led to product formation, however, limonene production was poor (Figure S2A). This is expected as IspA can perform both the first and second reactions in the formation of FPP diverting GPP away from limonene synthesis towards FPP accumulation (Ku et al., 2005). This could be alleviated in the future by using a more specific GPP synthase that only catalyzes the production of GPP rather than IspA (Alonso-Gutierrez et al., 2013). Overall, isoprenol proved to be a better substrate than prenol or the 3:1 isoprenol:prenol molar mix

(Figure S2A) leading us to focus on using isoprenol exclusively, in combination with IDI, for the subsequent optimization work. By observing the formation of pathway intermediates (Figure S2B), we could also see detectable levels of prenyl diphosphates within 1–2 hr.

3.3 | Optimization of enzyme levels for flux maximization

With a working system in hand, the concentrations of pathway intermediates from Figure S2B and the kinetic parameters in Table 1 were used to estimate a starting point for optimization of the multienzyme system. A perturbation experiment was designed whereby each enzyme concentration (CK, IPK, IDI, IspA, and GGPPS) was individually increased or decreased 5 fold while holding all other enzyme concentrations stationary at a midpoint (Figure 2a), the concentration of pathway intermediates was measured after 24 hr. The effects of changing each enzyme on the overall system were in some cases intuitive. For example, when the concentration of CK was increased the accumulation of its product, IP, increased, as it did when the concentration of the subsequent enzyme, IPK, which uses IP as a substrate was decreased (Figure 2b,c). Overall the midpoint concentration of each enzyme was found to be the best for the higher accumulation of GGPP (Figure 2b–f). To perform a more quantitative analysis of the effects of enzyme concentration and intermediate accumulation on the overall flux of the system, MCA was applied to this system. However, to do so, a greater number of perturbations was required and the formation of a pseudo-steady state (PSS), one of the underlying assumptions of MCA (Wu et al., 2004), needed to be confirmed. To identify a PSS, we ran an in vitro reaction, using the optimized enzyme concentrations, as predicted from the initial perturbation study, using a main effects linear regression model. The formation of intermediates over time using the optimized enzyme system was constructed and GGPP was found to increase linearly between 45–90 min (Figure S3), while all other intermediates remained steady during this time. Therefore, 60 min was chosen as the reaction time for the large perturbation study. Using this data (Table S3), the elasticities of each enzyme toward the pathway intermediates were calculated using the method developed by Wu et al. (2004). This framework is capable of accommodating large fluctuations in enzyme concentrations typically found in cell-free systems but rarely encountered in vivo systems, to which MCA is traditionally applied. The results are shown in Figure 3. Only five elasticities were found to be significant ($p < .05$): ε_{CK}^{IP}, ε_{IPK}^{IP}, ε_{IDI}^{IPP}, ε_{IDI}^{GPP}, and ε_{IspA}^{IPP}. This indicated that high IP concentrations were slightly inhibitory towards CK activity (Figure 3b), IP concentration increased significantly upon increasing CK concentration as is typical of the first committed step for a pathway and consistent with its role as a product of CK (Figure S4). IP was stimulatory for IPK activity (Figure 3c), which correlates well to its role as a substrate in this reaction. IPP/DMAPP concentration had a stimulatory effect on IDI and IspA both of which use IPP/DMAPP as substrates (Figure 3d,e). GGPPS concentration showed no effect on the overall pathway flux (Figure 3a) in the ranges tested nor were any of its elasticities significant (Figure 3f). We observed that the concentration of GGPPS could, therefore, be decreased a least 5 fold without any effect on the pathway flux and we thus used this new concentration of GGPPS in the following experiments.

3.4 | Optimization of process parameters for taxadiene production

Having identified the optimal enzyme concentrations, we sought to probe the operational limits of this process by conducting the remaining experiments with the above-optimized enzyme system, but now also including TDS (concentrations of the final optimized conditions are reported in the Section 2). First, based on the determined k_{cat} for TDS (Table 1), an excess of this enzyme (200 μg/ml) was added to the optimized multienzyme system and the reaction was monitored over time for linearity (Figure 4). After 2 hr, taxadiene production was found to be linear until at least 24 hr (Figure 4a). Therefore, the ratio of TDS to the rest of the enzyme system was optimized by varying the concentration of TDS and monitoring the concentration of taxadiene after 20 hr (Figure 4b). At concentrations of TDS above 20 μg/ml, taxadiene concentration was constant, therefore, a final concentration of 25 μg/ml of TDS was used in the following studies to probe the effects of cofactors on taxadiene production (Figure 5). Increasing either ATP or ADP concentrations in the reaction mixture had a negative effect on the taxadiene production (Figure 5a). With regard to ATP, taxadiene production increased as ATP increased until 10 mM after which, taxadiene production was abolished. Similarly, Chen et al. (2017) found that ATP levels above 5 mM completely inhibited the enzyme IspA, however, amorphadiene yields in their cell-free system increased in their multienzyme system when ATP was between 5–15 mM. This suggests that inhibition could be circumvented by increasing IspA concentration and thereby increasing the ratio of active sites in IspA to ATP molecules. Inhibition was also detected in our system when high concentrations of ADP were used (Figure 5a). Inhibition occurred earlier for ADP which was added in addition to 10 mM ATP. A possible explanation for this effect is the combined ionic strength of the two nucleotides which were added as sodium salts which could be causing a salting-out effect. In fact, a combined concentration of 20 mM of ATP and 20 mM ADP quickly resulted in the formation of a visible protein precipitate (<1 hr). As a result of this precipitation, ATP concentration becomes a limiting factor in the design of this system. Since 8 moles of ATP are required to synthesize 1 mole of taxadiene, this limits the maximum achievable taxadiene titer to 340 mg/L if 10 mM ATP is used. In the long term, this problem may be circumvented by using immobilized enzymes which are less susceptible to ionic strength. This would also have additional advantages of increasing the long-term stability of the enzymes and simplifying the downstream recovery of the isoprenoids. Alternatively, an ATP recycling system can be implemented which maintains the ATP concentration at the optimal level and uses a substrate with a lower ionic strength like polyphosphate. The

dependence of the reaction on dithiothreitol (DTT) and magnesium was characterized by titrating each reagent (Figure 5b). When magnesium was not added, very little taxadiene was detected. Presumably, some residual enzyme-bound magnesium from the cell was still present after purification. DTT also had a positive effect on the system's activity with an optimum around 2 mM.

Since the number of enzymes is a significant driver of production costs in cell-free synthesis processes (Lima-ramos, Nordblad, & Woodley, 2011), we wanted to explore the possibility of eliminating the enzyme IDI in the multienzyme system by supplying the proper ratio of IPP and DMAPP precursors isoprenol and prenol. Multienzyme assays were conducted without IDI with varying ratios of the substrates isoprenol and prenol (Figure 5c). Taxadiene production was highest when isoprenol was in excess of prenol and decreased with an increasing proportion of prenol added. This behavior is likely due to the increased stoichiometric need for IPP over DMAPP for taxadiene production (three IPP and one DMAPP) but also could be due to the preference of the enzymes CK for isoprenol and the preference of IPK for IP. Eliminating IDI also decreased the overall productivity by 58%, (24 mg/L vs. 14 mg/L). However, reoptimization of this system in the absence of IDI may alleviate this problem. Using the minimized enzyme system without IDI, taxadiene (five enzyme system), amorphadiene, valencene, and limonene (four enzyme systems) could all be synthesized using a 3:1 substrate ratio (Figure 5d).

3.5 | Determining the most significant factors for optimization using the ODE model

One of the goals of this work was to use the in vitro data to identify the promising avenues for optimization in the in vivo system. As MCA analysis did not reveal any unusual sensitivities, we determined the system's sensitivity to individual enzyme kinetic parameters to identify those enzymes which could be improved using an ODE model. The full details of the model development and all starting parameters used are given in the Supporting Information. The concentration of pathway intermediates over time is shown in Figure S5A-C and represents the scenario where enzyme concentrations are increased 10 fold over the optimal concentrations reported in Section 2.5. Global sensitivity analysis of all model variables including K_m, k_{cat}, and enzyme concentrations toward taxadiene production was performed using Monte Carlo simulations and multiple linear regression with stepwise elimination. Ten variables were found to be significant ($p < .01$, Figure S5D) four of which were enzyme concentrations (CK, TDS, IPK, GGPPS) and the remaining six variables related to the two condensation reactions which form GPP and FPP. These two reactions can be catalyzed by either IspA or GGPPS with IspA catalyzing the condensation of IPP and DMAPP as well as IPP and GPP. Furthermore, GGPPS derived from *T. canadensis* is also capable of catalyzing the condensation of 3 IPP and DMAPP, 2 IPP and GPP, and 1 IPP and FPP into GGPP with higher catalytic constant than IspA (Table 1). This suggests that the kinetics of these two intermediate steps are far more important than previously realized and should be the focus of future in vitro and in vivo studies.

3.6 | Optimized system is scalable and leads to high taxadiene titers

Ultimately, the overall objective of this work was the optimization of the IUP in vitro, which we wanted to demonstrate by achieving a high flux toward the diterpene taxadiene. To validate the time profiles generated from the ODE model, a time course of four different enzyme concentrations was constructed and compared with the predicted time course for taxadiene production (Figure 6a). The overall molar ratio of the enzymes was kept constant, however, the concentration of each enzyme was increased either 2, 5, or 10 fold over the baseline (See Section 2.5; 1×). Furthermore, to demonstrate the scalability of the system, the taxadiene productivity was predicted using the ODE model for enzymes concentrations between 0.1 and 40-fold increased from the baseline concentrations and compared with the experimental flux determined from the time course studies (Figure 6b). Further increases in enzyme concentrations are predicted by our model to increase the flux of the pathway even further Figure 6b, however, at higher enzyme concentrations, the high flux is sustained without minimizing enzyme usage, making any increases beyond a 10-fold increase in enzymes concentration less cost-effective in a homogenous system. Overall, we were able to produce 220 mg/L of taxadiene in just 9 hr, at a total flux of 24.4 $mg{\cdot}L^{-1}{\cdot}h^{-1}$, converting 65% of the available isoprenol and ATP to taxadiene, a 2.9-fold increase over the fastest flux (8.5 $mg{\cdot}L^{-1}{\cdot}h^{-1}$) ever reported for this diterpene (Ajikumar et al., 2010).

4 | CONCLUSION

Our investigation demonstrates that cell-free biosynthesis using the IUP is a promising route for the production of high-value complex cyclic diterpenoids like taxadiene. The IUP takes advantage of a low-cost feedstock, isoprenol, and uses a relatively small number of enzymes (five for diterpenes and four for mono- or sesquiterpenoids) compared with other cell-free systems for isoprenoid production (Korman et al., 2017). When compared with in vivo systems, cell-free production can sustain higher flux as there is no competition for precursors to support biological functions meaning theoretically all of the substrates could be converted into the product. Furthermore, due to its simplicity, this system could also be coupled with a large number of downstream pathways either for the commercial production of many different products or to study these pathways in more detail outside of the cell. Another significant advantage of the cell-free production of isoprenoids is the ease of recovery of the isoprenoids from the reaction media which can often account for a significant portion of the costs in vivo systems. The easy recovery along with the precise control of reaction conditions associated with cell-free systems might be particularly useful for synthesizing high purity reference standards for example.

The overall economic viability of the cell-free IUP platform will ultimately depend on the cost of enzyme purification and the long-term stability of the enzymes (Dudley et al., 2015). Immobilization studies and the implementation of an ATP regeneration system will

be necessary to reduce the overall ionic strength of the reaction media and maintain the long-term stability of these enzymes and will, therefore, be the subject of future investigations.

ACKNOWLEDGMENTS

We acknowledge discussions and input from Benjamin Woolston and Jason King. This project was supported by the Department of Energy grants DE-SC 000 8744 and DE-EE 000 7531. V.W. was supported by the Natural Sciences and Engineering Research Council, Canada.

CONFLICT OF INTERESTS

The authors are listed as inventors in a pending patent application (no. US 16/425,373; applicant, Massachusetts Institute of Technology) encompassing all the information presented here, as well as additional applications.

ORCID

Valerie C.A. Ward http://orcid.org/0000-0001-9784-3511
Alkiviadis Orfefs Chatzivasileiou http://orcid.org/0000-0003-1622-6680

REFERENCES

Ajikumar, P. K., Xiao, W. H., Tyo, K. E. J., Wang, Y., Simeon, F., Leonard, E., … Stephanopoulos, G. (2010). Isoprenoid pathway optimization for Taxol precursor overproduction in *Escherichia coli*. *Science*, *330*(2010), 70–74. https://doi.org/10.1126/science.1191652.

Alonso-Gutierrez, J., Chan, R., Batth, T. S., Adams, P. D., Keasling, J. D., Petzold, C. J., & Lee, T. S. (2013). Metabolic engineering of *Escherichia coli* for limonene and perillyl alcohol production. *Metabolic Engineering*, *19*, 33–41. https://doi.org/10.1016/j.ymben.2013.05.004.

Andexer, J. N., & Richter, M. (2015). Emerging enzymes for ATP regeneration in biocatalytic processes. *ChemBioChem*, *16*(3), 380–386. https://doi.org/10.1002/cbic.201402550

Boronat, A., & Rodríguez-Concepción, M. (2015). Terpenoid biosynthesis in prokaryotes. *Advances in Biochemical Engineering/Biotechnology*, *148*, 3–18.

Brostrom, M. A., & Browning, E. T. (1973). Choline kinase from brewers' yeast. Partial purification, properties, and kinetic mechanism. *The Journal of Biological Chemistry*, *248*(7), 2364–2371.

Burke, C., & Croteau, R. (2002). Interaction with the small subunit of geranyl diphosphate synthase modifies the chain length specificity of geranylgeranyl diphosphate synthase to produce geranyl diphosphate*. *Journal of Biological Chemistry*, *277*(5), 3141–3149. https://doi.org/10.1074/jbc.M105900200.

Chatzivasileiou, A. O., Ward, V., Edgar, S. M., & Stephanopoulos, G. (2019). Two-step pathway for isoprenoid synthesis. *Proceedings of the National Academy of Sciences*, *116*(2), 506–511. https://doi.org/10.1073/pnas.1812935116

Chen, X., Zhang, C., Zou, R., Stephanopoulos, G., & Too, H. P. (2017). In vitro metabolic engineering of amorpha-4,11-diene biosynthesis at enhanced rate and specific yield of production. *ACS Synthetic Biology*, *6*(9), 1691–1700. https://doi.org/10.1021/acssynbio.6b00377

Chen, Y., Zhou, Y. J., Siewers, V., & Nielsen, J. (2015). Enabling technologies to advance microbial isoprenoid production. *Advances in Biochemical Engineering/Biotechnology*, *148*, 143–160.

Dudley, Q. M., Karim, A. S., & Jewett, M. C. (2015). Cell-free metabolic engineering: Biomanufacturing beyond the cell. *Biotechnology Journal*, *10*, 69–82. https://doi.org/10.1002/biot.201400330

Galloway, D. A., Laimins, L. A., Division, B., & Hutchinson, F. (2015). In vitro reconsitution of metabolic pathways: Insights into nature's chemical logic. *Synlett*, *26*(8), 87–92. https://doi.org/10.1016/j.coviro.2015.09.001.Human

George, K. W., Thompson, M. G., Kim, J., Baidoo, E. E. K., Wang, G., Benites, V. T., … Lee, T. S. (2018). Integrated analysis of isopentenyl pyrophosphate (IPP) toxicity in isoprenoid-producing *Escherichia coli*. *Metabolic Engineering*, *47*(January), 60–72. https://doi.org/10.1016/j.ymben.2018.03.004

Guo, W., Sheng, J., & Feng, X. (2017). Mini-review: In vitro metabolic engineering for biomanufacturing of high-value products. *Computational and Structural Biotechnology Journal*, *15*, 161–167. https://doi.org/10.1016/j.csbj.2017.01.006

Guterl, J. K., Garbe, D., Carsten, J., Steffler, F., Sommer, B., Reiße, S., … Sieber, V. (2012). Cell-free metabolic engineering: Production of chemicals by minimized reaction cascades. *CHEM SUS CHEM*, *5*, 2165–2172. https://doi.org/10.1002/cssc.201200365

Hahn, F. M., Hurlburt, A. P., & Poulter, C. D. (1999). *Escherichia coli* open reading frame 696 is idi, a nonessential gene encoding isopentenyl diphosphate isomerase. *Journal of Bacteriology*, *181*(15), 4499–4504.

Kim, K. H., Voelker, D. R., & Carman, G. M. (1997). Expression, purification, and characterization of choline kinase, product of the CK1 gene from yeast. *FASEB Journal*, *11*(9), A1344–A1344.

Korman, T. P., Opgenorth, P. H., & Bowie, J. U. (2017). A synthetic biochemistry platform for cell free production of monoterpenes from glucose. *Nature Communications*, *8*(May), 1–8. https://doi.org/10.1038/ncomms15526

Ku, B., Jeong, J. C., Mijts, B. N., Schmidt-Dannert, C., & Dordick, J. S. (2005). Preparation, characterization, and optimization of an in vitro C30 carotenoid pathway. *Applied and Environmental Microbiology*, *71*(11), 6578–6583. https://doi.org/10.1128/AEM.71.11.6578-6583.2005

Lange, B. M., & Croteau, R. (1999). Isopentenyl diphosphate biosynthesis via a mevalonate-independent pathway: Isopentenyl monophosphate kinase catalyzes the terminal enzymatic step, 96(24).

Liebermeister, W., & Klipp, E. (2006). Bringing metabolic networks to life: Convenience rate law and thermodynamic constraints. *Theoretical Biology and Medical Modelling*, *3*(41), 3. https://doi.org/10.1186/1742-4682-3-41

Lima-ramos, J., Nordblad, M., & Woodley, J. M. (2011). Guidelines and Cost Analysis for Catalyst Production in Biocatalytic Processes Pa Abstract:, 15(1), 266–274.

Malhotra, K., Subramaniyan, M., Rawat, K., Kalamuddin, M., Qureshi, M. I., Malhotra, P., … Kumar, S. (2016). Compartmentalized metabolic engineering for artemisinin biosynthesis and effective malaria treatment by oral delivery of plant cells. *Molecular Plant*, *9*(11), 1464–1477. https://doi.org/10.1016/j.molp.2016.09.013

Martin, V. J. J., Pitera, D. J., Withers, S. T., Newman, J. D., & Keasling, J. D. (2003). Engineering a mevalonate pathway in *Escherichia coli* for production of terpenoids. *Nature Biotechnology*, *21*(7), 796–802. https://doi.org/10.1038/nbt833

Meadows, A. L., Hawkins, K. M., Tsegaye, Y., Antipov, E., Kim, Y., Raetz, L., … Tsong, A. E. (2016). Rewriting yeast central carbon metabolism for industrial isoprenoid production. *Nature*, *537*(7622), 694–697. https://doi.org/10.1038/nature19769

Mordhorst, S., Siegrist, J., Müller, M., Richter, M., & Andexer, J. N. (2017). Catalytic alkylation using a cyclic S-adenosylmethionine regeneration system. *Angewandte Chemie (International ed. in English)*, *56*, 4037–4041. https://doi.org/10.1002/anie.201611038

Schwander, T., Schada von Borzyskowski, L., Burgener, S., Cortina, N. S., & Erb, T. J. (2016). A synthetic pathway for the fixation of carbon dioxide in vitro. *Science (New York, N.Y.)*, *354*(6314), 900–904.

Vickers, C. E., Bongers, M., Liu, Q., Delatte, T., & Bouwmeester, H. (2014). Metabolic engineering of volatile isoprenoids in plants and microbes. *Plant, Cell & Environment*, *37*(8), 1753–1775. https://doi.org/10.1111/pce.12316

Wang, P. H., Khusnutdinova, A. N., Luo, F., Xiao, J., Nemr, K., Flick, R., … Yakunin, A. F. (2018). Biosynthesis and activity of prenylated FMN cofactors. *Cell Chemical Biology*, *25*(5), 560–570. https://doi.org/10.1016/j.chembiol.2018.02.007. e6

Wang, Y., & Zhang, Y. P. (2009). Cell-free protein synthesis energized by slowly-metabolized, 8, 1–8. https://doi.org/10.1186/1472-6750-9-58

Ward, V., Chatzivasileiou, A. O., & Stephanopoulos, G. (2018). Metabolic engineering of *Escherichia coli* for the production of isoprenoids. *FEMS Microbiology Letters*, *365*(10), fny079. https://doi.org/10.1093/femsle/fny079

Weaver, L. J., Sousa, M. M. L., Wang, G., Baidoo, E., Petzold, C. J., & Keasling, J. D. (2015). A kinetic-based approach to understanding heterologous mevalonate pathway function in *E. coli*. *Biotechnology and Bioengineering*, *112*(1), 111–119. https://doi.org/10.1002/bit.25323

Wu, L., Wang, W., Van Winden, W. A., Van Gulik, W. M., & Heijnen, J. J. (2004). A new framework for the estimation of control parameters in metabolic pathways using lin-log kinetics. *European Journal of Biochemistry*, *271*, 3348–3359. https://doi.org/10.1111/j.1432-1033.2004.04269.x

Yang, G., Sau, C., Lai, W., Cichon, J., & Li, W. (2015). Distributing a metabolic pathway among a microbial consortium enhances production of natural products. *Nature Biotechnology*, *33(4)*(4), 377–383. https://doi.org/10.1126/science.1249098.Sleep

Zhang, Y. H. P. (2011). Simpler is better: High-yield and potential low-cost biofuels production through cell-free synthetic pathway biotransformation (SyPaB). *ACS Catalysis*, *1*(9), 998–1009. https://doi.org/10.1021/cs200218f

Zhu, F., Zhong, X., Hu, M., Lu, L., Deng, Z., & Liu, T. (2014). In vitro reconstitution of mevalonate pathway and targeted engineering of farnesene overproduction in *Escherichia coli*. *Biotechnology and Bioengineering*, *111*(7), 1396–1405. https://doi.org/10.1002/bit.25198

SUPPORTING INFORMATION

Additional supporting information may be found online in the Supporting Information section.

How to cite this article: Ward VC, Chatzivasileiou AO, Stephanopoulos G. Cell free biosynthesis of isoprenoids from isopentenol. *Biotechnol. Bioeng.* 2019;1–13. https://doi.org/10.1002/bit.27146